Femtosecond laser written waveguides with MoS_2 as satuable absorber for passively Q-switched lasing

Chen Cheng,[1] Hongliang Liu,[1] Zhen Shang,[1] Weijie Nie,[1] Yang Tan,[1] Blanca del Rosal Rabes,[2] Javier R. Vázquez de Aldana,[3] Daniel Jaque,[2] and Feng Chen[1,*]

[1]*School of Physics, State Key Laboratory of Crystal Materials and Key Laboratory of Particle Physics and Particle Irradiation (MOE), Shandong University, Jinan 250100, China*

[2]*Fluorescence Imaging Group, Departamento de Física de Materiales, Facultad de Ciencias, Universidad Autónoma de Madrid, Madrid 28049, Spain*

[3]*Laser Microprocessing Group, Universidad de Salamanca, Salamanca 37008, Spain*

[*]*drfchen@sdu.edu.cn*

Abstract: This work reports on the passively Q-switched waveguide laser system based on Nd:YAG crystal and MoS_2 satuable absorber. A depressed cladding waveguide with circular cross-sectional geometry has been produced in Nd:YAG crystal by direct femtosecond laser writing at low-repetition rate. The confocal microscopic investigation of the structure reveals the well-preserved microphotoluminescence features in the waveguide core. With chemical-vapor-deposition (CVD) MoS_2 membrane as satuable absorber, the passive Q-switching of the Nd:YAG waveguide system has been achieved under optical pump, reaching maximum average output power of 85.2 mW, corresponding to single-pulse energy of 112 nJ, at wavelength of 1064 nm. The repetition rate of the pulsed waveguide laser system is tunable from 0.51 to 1.10 MHz, and the obtained minimum pulse duration is 203 ns.

OCIS codes: (230.7370) Waveguidse; (140.3540) Lasers, Q-switched; (140.3390) Laser materials processing.

References and links

1. A. Peruzzo, M. Lobino, J. C. F. Matthews, N. Matsuda, A. Politi, K. Poulios, X. Q. Zhou, Y. Lahini, N. Ismail, K. Wörhoff, Y. Bromberg, Y. Silberberg, M. G. Thompson, and J. L. OBrien, "Quantum Walks of Correlated Photons," Science **329**(5998), 1500–1503 (2010).
2. A. Schaap, Y. Bellouard, and T. Rohrlack, "Optofluidic lab-on-a-chip for rapid algae population screening," Biomed. Opt. Express **2**(3), 658–664 (2011).
3. Y. Liao, J. Song, E. Li, Y. Luo, Y. Shen, D. Chen, Y. Cheng, Z. Xu, K. Sugioka, and K. Midorikawa, "Rapid prototyping of three-dimensional microfluidic mixers in glass by femtosecond laser direct writing," Lab Chip **12**(4), 746–749 (2012).
4. D. Choudhury, J. R. Macdonald, and A. K. Kar, "Ultrafast laser inscription: perspectives on future integrated applications," Laser Photonics Rev. **8**(6), 827–846 (2014).
5. Y. Tan, S. Akhmadaliev, S. Zhou, S. Sun, and F. Chen, "Guided continuous-wave and graphene-based Q-switched lasers in carbon ion irradiated Nd:YAG ceramic channel waveguide," Opt. Express **22**(3), 3572–3577 (2014).
6. E. J. Murphy, *Intergrated Optical Circuits and Components* (Marcel Dekker, 1999).
7. T. Calmano and S. Müller, "Crystalline Waveguide Lasers in the Visible and Near-Infrared Spectral Range," IEEE J. Sel. Top. Quantum Electron. **21**(1), 401 (2015).
8. F. Chen and J. R. Vazquez de Aldana, "Optical waveguides in crystalline dielectric materials produced by femtosecond-laser micromachining," Laser Photonics Rev. **8**(2), 251–275 (2014).
9. W. Nie, C. Cheng, Y. Jia, C. Romero, J. R. Vázquez de Aldana, and F. Chen, "Dual-wavelength waveguide lasers at 1064 and 1079 nm in Nd:YAP crystal by direct femtosecond laser writing," Opt. Lett. **40**(10), 2437–2440 (2015).
10. K. Hasse, T. Calmano, B. Deppe, C. Liebald, and C. Kränkel, "Efficient Yb^{3+}:$CaGdAlO_4$ bulk and femtosecond-laser-written waveguide lasers," Opt. Lett. **40**(15), 3552–3555 (2015).
11. Y. Tan, C. Zhang, F. Chen, F. Q. Liu, D. Jaque, and Q. M. Lu, "Room-temperature continuous wave laser oscillations in Nd:YAG ceramic waveguides produced by carbon ion implantation," Appl. Phys, B-Lasers O. **103**(4), 837–840 (2011).

#255483 Received 9 Dec 2015; revised 23 Dec 2015; accepted 4 Jan 2016; published 6 Jan 2016

12. Y. Jia, C. Cheng, J. R. Vázquez de Aldana, G. R. Castillo, B. R. Rabes, Y. Tan, D. Jaque, and F. Chen, "Monolithic crystalline cladding microstructures for efficient light guiding and beam manipulation in passive and active regimes," Sci. Rep. **4**, 5988 (2014).
13. K. M. Davis, K. Miura, N. Sugimoto, and K. Hirao, "Writing waveguides in glass with a femtosecond laser," Opt. Lett. **21**(21), 1729–1731 (1996).
14. R. R. Gattass and E. Mazur, "Femtosecond laser micromachining in transparent materials," Nat. Photonics **2**(4), 219–225 (2008).
15. Y. Liao, Y. Shen, L. Qiao, D. Chen, Y. Cheng, K. Sugioka, and K. Midorikawa, "Femtosecond laser nanostructuring in porous glass with sub-50 nm feature sizes," Opt. Lett. **38**(2), 187–189 (2013).
16. R. Osellame, G. Cerullo, and R. Ramponi, *Femtosecond LaserMicromachining: Photonic and Microfluidic Devices in Transparent Materials* (Springer, 2012).
17. G. Douglass, F. Dreisow, S. Gross, S. Nolte, and M. J. Withford, "Towards femtosecond laser written arrayed waveguide gratings," Opt. Express **23**(16), 21392–21402 (2015).
18. N. Pavel, G. Salamu, F. Jipa, and M. Zamfirescu, "Diode-laser pumping into the emitting level for efficient lasing of depressed cladding waveguides realized in Nd:YVO4 by the direct femtosecond-laser writing technique," Opt. Express **22**(19), 23057–23065 (2014).
19. G. C. Righini and A. Chiappini, "Glass optical waveguides: a review of fabrication techniques," Opt. Eng. **53**(7), 071819 (2014).
20. M. Ams, G. D. Marshall, P. Dekker, J. A. Piper, and M. J. Withford, "Ultrafast laser written active devices," Laser Photonics Rev. **3**(6), 535–544 (2009).
21. N. Pavel, G. Salamu, F. Voicu, F. Jipa, M. Zamfirescu, and T. Dascalu, "Efficient laser emission in diode-pumped Nd:YAG buried waveguides realized by direct femtosecond-laser writing," Laser Phys. Lett. **10**(9), 095802 (2013).
22. J. Martinez de Mendivil, J. Hoyo, J. Solis, M. C. Pujol, M. Aguiló, F. Diaz, and G. Lifante, "Channel waveguide fabrication in $KY(WO_4)_2$ combining liquid-phase-epitaxy and beam-multiplexed femtosecond laser writing," Opt. Mater. **47**, 304–309 (2015).
23. Y. Jia, Y. Tan, C. Cheng, J. R. Vázquez de Aldana, and F. Chen, "Efficient lasing in continuous wave and graphene Q-switched regimes from Nd:YAG ridge waveguides produced by combination of swift heavy ion irradiation and femtosecond laser ablation," Opt. Express **22**(11), 12900–12908 (2014).
24. H. Liu, C. Cheng, C. Romero, J. R. Vázquez de Aldana, and F. Chen, "Graphene-based Y-branch laser in femtosecond laser written Nd:YAG waveguides," Opt. Express **23**(8), 9730–9735 (2015).
25. Y. Y. Ren, G. Brown, R. Mary, G. Demetriou, D. Popa, F. Torrisi, A. C. Ferrari, F. Chen, and A. K. Kar, "7.8-GHz Graphene-Based 2-um Monolithic Waveguide Laser," J. Sel. Top. Quant. Electron. **21**, 1 (2015).
26. Y. Tan, R. He, C. Cheng, D. Wang, Y. Chen, and F. Chen, "Polarization-dependent optical absorption of MoS_2 for refractive index sensing," Sci. Rep. **4**, 7523 (2014).
27. Y. X. Li, N. N. Dong, S. F. Zhang, X. Y. Zhang, Y. Y. Feng, K. P. Wang, L. Zhang, and J. Wang, "Giant two-photon absorption in monolayer MoS_2," Laser Photonics Rev. **9**(4), 427–434 (2015).
28. R. I. Woodward, R. C. T. Howe, G. Hu, F. Torrisi, M. Zhang, T. Hasan, and E. J. R. Kelleher, "Few-layer MoS_2 saturable absorbers for short-pulse laser technology: current status and future perspectives Invited," Photonics Res. **3**(2), A30–A42 (2015).
29. B. L. Wang, H. H. Yu, H. Zhang, C. J. Zhao, S. C. Wen, H. J. Zhang, and J. Y. Wang, "Topological Insulator Simultaneously Q-Switched Dual-Wavelength Nd:Lu_2O_3 Laser," IEEE Photonics J. **6**, 1501007 (2014).
30. X. Liu and Y. Cui, "Flexible pulse-controlled fiber laser," Sci. Rep. **5**, 9399 (2015).
31. Y. Chen, G. Jiang, S. Chen, Z. Guo, X. Yu, C. Zhao, H. Zhang, Q. Bao, S. Wen, D. Tang, and D. Fan, "Mechanically exfoliated black phosphorus as a new saturable absorber for both Q-switching and Mode-locking laser operation," Opt. Express **23**(10), 12823–12833 (2015).
32. S. Wang, H. Yu, H. Zhang, A. Wang, M. Zhao, Y. Chen, L. Mei, and J. Wang, "Broadband Few-Layer MoS2 Saturable Absorbers," Adv. Mater. **26**(21), 3538–3544 (2014).
33. J. Du, Q. Wang, G. Jiang, C. Xu, C. Zhao, Y. Xiang, Y. Chen, S. Wen, and H. Zhang, "Ytterbium-doped fiber laser passively mode locked by few-layer Molybdenum Disulfide (MoS_2) saturable absorber functioned with evanescent field interaction," Sci. Rep. **4**, 6346 (2014).
34. H. Zhang, S. B. Lu, J. Zheng, J. Du, S. C. Wen, D. Y. Tang, and K. P. Loh, "Molybdenum disulfide (MoS_2) as a broadband saturable absorber for ultra-fast photonics," Opt. Express **22**(6), 7249–7260 (2014).
35. R. I. Woodward, E. J. R. Kelleher, R. C. T. Howe, G. Hu, F. Torrisi, T. Hasan, S. V. Popov, and J. R. Taylor, "Tunable Q-switched fiber laser based on saturable edge-state absorption in few-layer molybdenum disulfide (MoS_2)," Opt. Express **22**(25), 31113–31122 (2014).
36. A. Choudhary, S. J. Beecher, S. Dhingra, B. D'Urso, T. L. Parsonage, J. A. Grant-Jacob, P. Hua, J. I. Mackenzie, R. W. Eason, and D. P. Shepherd, "456-mW graphene Q-switched Yb:yttria waveguide laser by evanescent-field interaction," Opt. Lett. **40**(9), 1912–1915 (2015).
37. S. Y. Choi, T. Calmano, M. H. Kim, D. I. Yeom, C. Kränkel, G. Huber, and F. Rotermund, "Q-switched operation of a femtosecond-laser-inscribed Yb:YAG channel waveguide laser using carbon nanotubes," Opt. Express **23**(6), 7999–8005 (2015).
38. A. Rodenas, G. A. Torchia, G. Lifante, E. Cantelar, J. Lamela, F. Jaque, L. Roso, and D. Jaque, "Refractive index change mechanisms in femtosecond laser written ceramic Nd:YAG waveguides: micro-spectroscopy experiments and beam propagation calculations," Appl. Phys, B-Lasers Opt. **95**(1), 85–96 (2009).

#255483 Received 9 Dec 2015; revised 23 Dec 2015; accepted 4 Jan 2016; published 6 Jan 2016

39. A. Benayas, W. F. Silva, C. Jacinto, E. Cantelar, J. Lamela, F. Jaque, J. R. Vázquez de Aldana, G. A. Torchia, L. Roso, A. A. Kaminskii, and D. Jaque, "Thermally resistant waveguides fabricated in Nd:YAG ceramics by crossing femtosecond damage filaments," Opt. Lett. **35**(3), 330–332 (2010).

1. Introduction

Optical waveguides have been widely applied in a broad range of areas, such as optical telecommunications, quantum computing, biophotonic sensing, and information processing, etc [1–6]. Recently, optically pumped solid-state waveguide lasers, serving as intriguing miniature light sources, have attracted more and more attentions due to a number of advantages of the systems [7–10]. Based on the compact waveguiding geometries, enhanced intracavity intensities in the waveguide cores enable more efficient generation of lasers in gain media [8, 11]. In addition, the small scale of the waveguide components matches the diameters of optical fibers, which shows the potential capability to construct complex photonic systems based on the waveguide chips and fibers [12].

Direct femtosecond laser writing/inscription has emerged as a powerful technique to fabricate waveguide devices in transparent optical materials [13–18]. Due to the efficient micro-engineering of the refractive index of the focal planes induced by the femtosecond laser pulses, either positive or negative index modifications could be achieved, resulting in the implementation of waveguiding structures with diverse configurations [8, 19]. In Nd:YAG laser crystal, a number of applications have been obtained based on the platform of laser-written waveguides, e.g., waveguide splitters and modulators in passive regime, and waveguide amplifications and lasers in active regime [12, 20, 21]. Owing to the excellent fluorescence, physical and thermal properties, the Nd:YAG crystal has widely deployed to solid-state lasers as gain media. With Nd:YAG as the gain media, waveguide lasers have been realized in a mass of compact continuous-wave (CW) systems manufactured by epitaxial growth, ion beam implantation/irradiation, and femtosecond laser writing [22, 23]. Pulsed lasers on waveguide platforms permit compact cavity design with high optical intensities, which are intriguing light sources for on-chip integration [24, 25].

MoS_2 (molybdenum disulfide) is a novel two-dimensional (2D) nanomaterial, which consists of two hexagonal planes of S atoms coordinated through ionic-covalent interactions with the Mo atoms. It has distinctive electronic, optical, and catalytic properties with the geometry of the ultrathin layer, indicating interesting applications for electronic and optical devices [26, 27]. The saturable absorption (SA) is one of the most significant characteristics for MoS_2 as a member of nanosheet materials [28]. Owing to the SA feature, other nanomaterials, e.g., carbon nanotubes, black phosphorus, and graphene, have been successfully applied towards various applications in pulsed laser systems [24, 29–31]. With MoS_2 bulk as well as few-layer nanoplate as the SA in solid-state laser systems, pulsed lasers have obtained based on fibers and bulk materials [32–34]. In consideration of the bandgap of laminar MoS_2 nanosheet, the theories based on edge/defect state absorption can extended the bandgap from visible/near-visible spectral region to the near-infrared (NIR), enriching applications of solid laser systems with MoS_2 SA [35]. Nevertheless, in solid-state waveguide frameworks, the Q-switched lasers have not been achieved using MoS_2 as SA in the systems, although a few works have been performed on the SA via graphene or carbon nanotubes [36, 37].

In this work, we report on the lasing characteristics, by employing a CVD MoS_2 thin film as SA, in Q-switched regimes of a laser written Nd:YAG cladding waveguide, of which the details have been investigated by a confocal micro-photoluminescence spectroscopy.

2. Experimental details

The Nd:YAG crystal (doped by 1 at.% Nd^{3+} ions) sample used in this work was cut into a wafer with dimension of $10 \times 9 \times 2$ mm^3 and optically polished. An amplified Ti:Sapphire laser system, to generate linearly-polarized 120 fs pulses at a central wavelength of 800 nm with 1 kHz repetition rate, was utilized to write the depressed cladding waveguides with the facility of Universidad de Salamanca, Spain. The pulse energy for micro-process was set with

#255483 Received 9 Dec 2015; revised 23 Dec 2015; accepted 4 Jan 2016; published 6 Jan 2016

a calibrated neutral density filter, a half-wave plate and a linear polarizer. The beam of fabricated fs laser was focused by the largest sample surface (10 × 9 mm^2) at a depth of 150 μm through a microscope objective (Leica 40 × , N.A. = 0.65) with a pulse energy of 2.52 μJ. The wafer was placed on a motorized 3-axes stage controlled by computer programming and drove with a constant speed of 0.5 mm/s during the irradiation along the direction perpendicular to both the fs laser propagation and the polarization. The parallel scans of cladding structure (with ~3 μm separation between adjacent tracks) were performed at different depths of the sample (from bottom to top of the sample in order to avoid the previously written tracks shielding the incident pulses), which consist of cladding structure. The cross sections of the cladding guiding structures in the Nd:YAG wafer can be seen in Fig. 1(a).

The homemade confocal microscope was used for the micro-fluorescence investigation of the waveguides. The 488-nm CW laser, as the optical excitation source, was focused in the sample by a 50 × microscope objective (N.A. ~0.55), yielding a spot with a diameter of approximately 0.53 μm. The subsequent emission of Nd^{3+} ions was collected by the same microscope objective, after passing through filters, lenses and pinholes, and was analyzed by a high resolution spectrometer. The software LabSpec and WSx were utilized to analyze and fit the spectra and process the fluorescence images in terms of the spectral intensity, energy shift and width of the fluorescence lines.

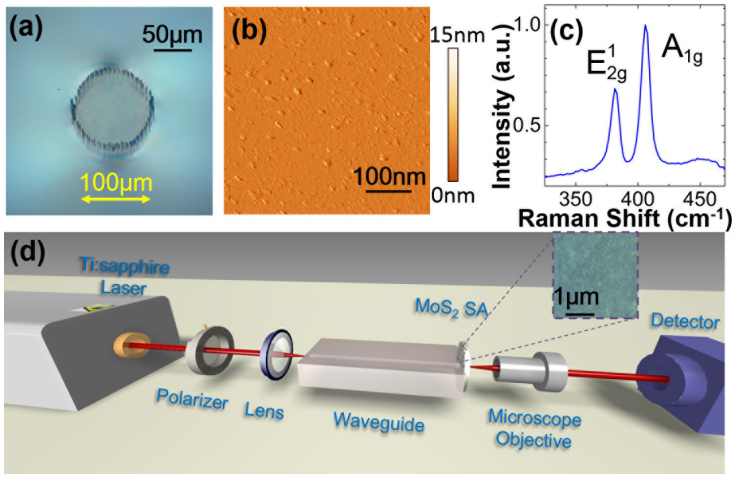

Fig. 1. Optical images of the fs laser micromachining cladding waveguides with the diameters of 100 μm (a). Schematic of the experimental setup for the pulsed waveguide laser (b). The inset picture is the microphotograph of the MoS_2 surface.

The CVD MoS_2 film coated glass wafer was a commercial product. The surface topography is characterized by an AFM (shown in Fig. 1(b)). The Raman spectrum of MoS_2 nanosheet depicted the shifted peaks appearing at 406 cm^{-1} and 381 cm^{-1}, which were corresponding to the in-plane E1 2g vibration mode and out-plane A_{1g} vibration mode, respectively (Fig. 1(c)). For ensuring the spatial integrity of the film, hybrid monolayer and few-layer (approximately 2~3 layers) of MoS_2 membrane consisted of the whole film. The Q-switching of waveguide lasing was realized by using an end-pump system. We utilized a linearly polarized light beam at 808 nm generated from a tunable CW Ti:Sapphire laser (Coherent MBR PE) as the pump source. A convex lens with a focal length of 30mm was used to couple the pump laser beam into the waveguide. A thin film was coated on end face towards the pump source with parameters of high reflectivity at ~1064nm and high transmission at ~808nm. The MoS_2 film was set as an output coupler mirror, by exerting mechanical bindings to make sure the SA was closely attached to the output facet of waveguides. The inset in Fig. 1(d) shows the microphotograph of the MoS_2 SA surface. It was 1000 × magnified and imaged by the optical microscope (Axio Imager, Carl Zeiss) operating

#255483 Received 9 Dec 2015; revised 23 Dec 2015; accepted 4 Jan 2016; published 6 Jan 2016

in reflection mode. The generated waveguide lasers were collected by utilizing a 20 × microscope objective lens (N.A. = 0.4) and imaged by using an infrared CCD. We used a spectrometer with resolution of 0.2 nm to analyze the emission spectra of the laser beam from the waveguide. The schematic plot of the experimental setup for the pulsed laser oscillations are depicted in Fig. 1(d).

3. Results and discussion

The modifications of the fs-laser inscription in the waveguide with 100μm-diameter have been shown in the fluorescence images included in Figs. 2, which illustrated modified the micro-structural and fluorescence properties in the filaments (fs laser focus). Figures 2(a)-2(c) shows the 2D spatial distributions of intensity, induced energy shift, as well as FWHM of the $^4F_{3/2}\rightarrow{}^4I_{9/2}$ inter-Stark level emission line of Nd^{3+} ions around 940 nm (this line has been found to be hyper-sensitive to slight changes in the Nd^{3+} environment, such as damage, volume changes and disorder) [8, 38, 39]. Figure 2(a) shows that the fluorescence intensity generated by Neodymium ions is significantly reduced at the laser irradiated volumes. This fact unequivocally reveals the efficient creation of defects at the waveguide contour (i.e. partially damaged areas) as a result of the localized optical breakdown. And it is further supported by the fluorescence image obtained in terms of the spatial variation of the fluorescence linewidth (Fig. 2(c)) that reveals a clear increment in the lattice disorder at the damage tracks. Laser irradiation does not only lead to the appearance of well-localized and disorder in the YAG network. The fluorescence map obtained in terms of the induced spectral shift of emission line reveals a remarkable luminescence shift towards lower energies (red-shift) at the waveguide contour (damage tracks) that, according to previous works, could be attributed to a local lattice compression at damage tracks. It is worth noting that this well agrees with previous works dealing with femtosecond fabrication of waveguides in YAG crystals and ceramics. It seems that the network damage created at the focal volume is companied by a relevant lattice compression that, in turns, is mechanically compensated by the appearance of dilated volumes located at the apex of damage filaments. Such mechanical compensation is also evidenced in the fluorescence map of Fig. 2(b) where a slight shift towards larger energies is observed at the bottom of the structure. The results in Fig. 2 reveal that a locally modification has been induced in a relevant damage only at the waveguide contour and the fluorescence properties at waveguide volume are well preserved.

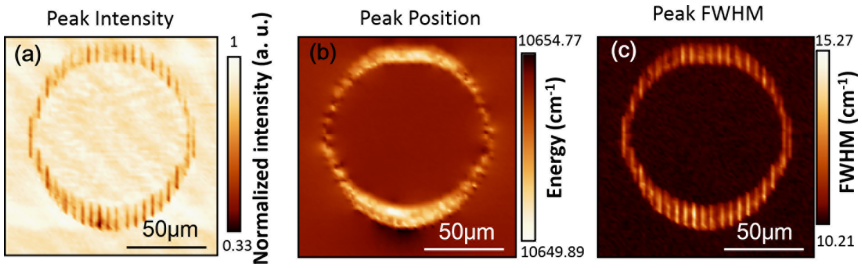

Fig. 2. 2D spatial dependence of the intensity (a), energy (b) and FWHM (c) corresponding to the $^4F_{3/2}\rightarrow{}^4I_{9/2}$ inter-Stark level emission line of Nd^{3+} in the waveguide region.

Figure 3(a) illustrates the average output power of Nd:YAG 1064 nm Q-switched waveguide laser as a function of absorbed pump power at 808 nm employing a glass sheet with MoS_2 thin film coated as SA. From the linear fit of the experiment data, we have determined that the slope efficiency (η) and lasing max average output power (P) are 23.9% (24.8%) and 83.3 mW (84.0 mW) at TM (TE) polarized light pump. The typical oscilloscope traces of the Q-switched pulse trains, of the waveguide at absorbed 616 mW TE- and TM-polarized pump light have been shown in Figs. 3(b) and 3(c) respectively. The bandwidth of the oscilloscope is 1 GHz and the minimum resolution of the detector is 0.2 ns. The waveguide contours are surrounded by strip tracks instead of symmetrical circle. Thereby, the slight inconformity of the trains indicated at TE- and TM-polarized pumped light is detected

#255483 Received 9 Dec 2015; revised 23 Dec 2015; accepted 4 Jan 2016; published 6 Jan 2016

by the reason of absorbed non-uniform at different orientations of pumped light. Figure 3(d) shows the laser emission spectrum from Nd:YAG waveguide at room temperature, as the absorbed pump power is above the oscillation threshold. The central wavelength for the Q-switched pulsed waveguide lasers is ~1063.9 nm, which clearly denote the laser oscillation line that corresponds to the main fluorescence of $^4F_{3/2} \rightarrow {}^4I_{11/2}$ transition of Nd^{3+} ions, the full width at half maximum (FWHM) value of this spectrum is about 0.4 nm. The inset two images present waveguide modal profiles of lasers at ~1064nm for TE- and TM- polarization. The average output power of the Q-switched waveguide laser was 83.3 mW and 84.0 mW along TM and TE polarizations, respectively. The corresponding energy of single pulse was 89 nJ. The pulse duration and repetition rate was 203 ns and 1.10 MHz, respectively. By varying the pumping power, the repetition rate of the waveguide pulsed laser could be tuned from 0.51 MHz to 1.10 MHz, as the absorbed power increases from 447 to 617 mW(see Figs. 4(a) and 4(b)). The more compact size of the waveguide laser system may be used as miniature light sources in photonic chips for diverse applications.

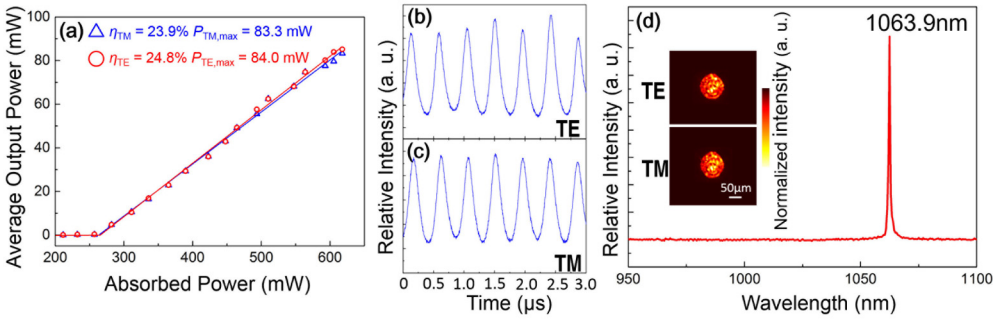

Fig. 3. The average output power (a) and the pulse trains (b, c) of the Q-switched waveguide lasers at TE- and TM- polarized light pump. Laser emission spectra form the Nd:YAG pulsed waveguide laser (d). The inset pictures show the output modal profiles from waveguide at TE- and TM-polarized light pump.

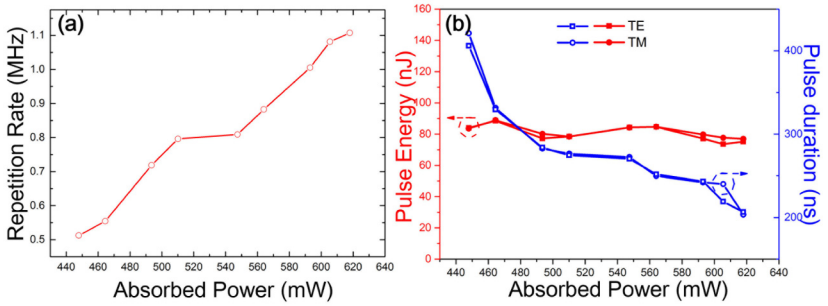

Fig. 4. The Q-switched laser repetition rate (a), pulse energy and duration (b) as functions of absorbed power.

4. Summary

In conclusion, by using MoS_2 as SA, the Q-switched waveguide lasers at 1064nm have been implemented in laser written Nd:YAG depressed cladding waveguide. The pulsed waveguide laser have a repetition rate ranging from 0.51 MHz to 1.10 MHz, with max average power of 84.0 mW, pulse energy of up to 89 nJ and minimum pulse duration of 203 ns. This work paves the way of MoS_2 based solid state waveguide lasers for photonic applications.

#255483 Received 9 Dec 2015; revised 23 Dec 2015; accepted 4 Jan 2016; published 6 Jan 2016

Acknowledgments

The work is supported by the National Natural Science Foundation of China (No. 11274203) and Junta de Castilla y León under Project SA086A12-2. Support from the Centro de Láseres Pulsados (CLPU) is also acknowledged.

#255483 Received 9 Dec 2015; revised 23 Dec 2015; accepted 4 Jan 2016; published 6 Jan 2016